Geometric Perception of the Brain: A Classical Approach Using Image Segmentation

J. Leite[1(✉)], P. A. Salgado[1], T.-P. Azevedo Perdicoúlis[1], and P. Lopes dos Santos[2]

[1] Escola de Ciências e Tecnologia, Universidade de Trás-os-Montes e Alto Douro, Vila Real 5000-811, Portugal
joanaalvesleite@gmail.com, {psal,tazevedo}@utad.pt
[2] Faculdade de Engenharia da Universidade do Porto, Porto 4200-465, Portugal
pjsantos@fe.up.pt

Abstract. This work focuses on the application of image processing techniques to segment and analyze images of brain sections with the aim of facilitating early diagnosis of brain tumors. The aim is to delineate specific regions of the brain, such as the cranial, intracranial, and encephalic regions, for subsequent geometric analysis. The process involves image pre-processing, conversion to polar coordinates, determination of contour points, Fourier Series approximation, and the use of the Least Square Method to obtain accurate representations of the regions. The proposed approach was tested on Magnetic Resonance Images of three different brains, showing its capability to accurately delineating the targeted regions. The results highlight the potential of signal processing techniques for analyzing brain images and provide insights for further research in this area.

Keywords: Medical Imaging · Pre-processing · Image Segmentation · Image Analysis

1 Introduction

Several fields of scientific knowledge have tried to assist medicine and healthcare along the years. Currently, complementary diagnostic tools have become indispensable in modern medicine due to the crucial additional information they offer, which might be unattainable through traditional conventional methods. Medical Imaging is undoubtedly one of the most relevant means in this context and can be analyzed through visualization systems or viewers [1]. While general image processing often emphasises aesthetics or create art, medical image

T-P. A. Perdicoúlis—Supported by FCT - Fundação para a Ciência e a Tecnologia under project UIDB/50014/2020 IDB/00048/2020
P. L. dos Santos—Supported by FCT - Fundação para a Ciência e a Tecnologia under project UIDB/50014/2020.

A. Cunha et al. (Eds.): MobiHealth 2023, LNICST 578, pp. 3–16, 2024.
https://doi.org/10.1007/978-3-031-60665-6_1

processing solely focuses on improving or artistic creativity, medical image is dedicated exclusively to enhancing the interpretability of displayed content. Its objectives include enhancing the image itself to highlight specific features and extracting information either through automated or manual means. The following classification outlines key categories for further exploration:

- Image enhancement: This involves removing image distortions like noise and background irregularities, as well as enhancing image contours and other relevant properties.
- Image segmentation: Its purpose is to demarcate the boundaries or contours of anatomical structures such as organs, vessels, or tumor lesions.
- Quantification: This category involves determining geometric properties of anatomical structures (e.g., perimeter, area, diameter, curvature) or physiological properties like perfusion characteristics or tissue composition.
- Computer-aided detection: The objective is to detect and characterize pathological structures and lesions, such as tumor lesions or vessel obstructions [2].

Medical Imaging, serving as a supplementary diagnostic tool, has evolved beyond mere visualization techniques and in-depth explorations of the human anatomy. This field enables the acquisition of information on the physiology and anatomy of internal organs non-invasively, using a variety of contemporary techniques, such as Magnetic Resonance Imaging (MRI), X-ray, Computed Tomography (CT) and Positron Emission Tomography (PET). These methodologies enable early detection of diseases, better coordination of medical treatments and even better general knowledge of the molecular activity of living organisms [3]. In Neuroscience, research extends beyond studying structure, volume, and morphometry. It also delves into understanding complex human mental processes, like language and consciousness, using tools such as MRI and (Functional MRI) fMRI [4]. These are important tools to support diagnosis, allowing specialists an in-depth study of pathologies of the nervous system and human behavior [5,6].

Medical images capture representations of the human body at various scales, ranging from microscopic to macroscopic. “ original:” They come in a wide variety of imaging modalities (e.g. a CT scanner, an ultrasound machine, etc.) and measure a physical property of the human body (e.g. radio-density, the opacity to X-rays). Available in diverse imaging modalities, such as CT scanners or ultrasound machines, they measure specific physical properties of the body, like radio-density or X-ray opacity. Specialized experts, like radiologists, interpret these images for clinical purposes, such as diagnostics, profoundly influencing physicians’ decision-making. Computer vision methods have long been employed to automatically analyze medical images. The recent advent of deep learning has replaced many other machine learning methods because it avoids the creation of hand-engineering features, thus removing a critical source of error from the process [7].

The mammalian nervous system consists of two divisions called the Central Nervous System (CNS) and peripheral nervous system (PNS). The CNS is formed by the brain and spinal cord, while the PNS includes nerve cells and

receptors outside. When observing an image of the nervous system, we realize that, with rare exceptions, all its structures occur in pairs, one on the left side and the other on the right side, that is, the left side is a specular image of the right side if you divide it into symmetrical halves—bilateral cerebral symmetry [8]. When referring to the CNS, it is common to use the terms white matter and gray matter. These terms arise due to the outermost layer of the brain being of gray color and mainly formed by neurons, while the innermost brain region is of white color, which is due to the myelin that coats these fibers, and consists mainly of nerve fibers (dendrites and axons).

The brain is the organ of the nervous system that is contained in the skull. It is the largest mass of nerve tissue in the body, and contains literally billions of nerve cells. The brain consists of three parts: the brain, the cerebellum and the brainstem [9]. Brain tumors are lesions representing alterations in brain tissues, which can include inflammation, bleeding, infections, or necrosis. These tumors result from the uncontrolled or excessive proliferation of either normal or aberrant cells. Based on their malignancy, tumors can be benign (noncancerous) or malignant (cancerous). Primary tumors can be malignant or benign and originate in the brain, whereas metastatic tumors are malignant, originate from other organs and spread to the brain through the bloodstream. Factors such as growth rate, distinct boundaries, and the ability to spread are considered to distinguish between benign and malignant primary brain tumors. Benign tumors have slow growth and rarely spread, while malignant tumors have rapid growth, are infiltrative and can be fatal [10]. Early detection of malignant tumors is paramount. Hence, technological solutions that can automatically delineate atypical brain regions are particularly valuable during the initial stages of diagnosis.

In this study, we introduce an innovative method for segmenting brain MRI images, which employs a geometric approximation technique based on the Fourier Series (FS), in view to facilitate diagnosis and consequent early detection of brain tumors. Classic approaches of image processing are applied to several images of the horizontal section of brains to perform the segmentation of these images.This procedure targets delineation of specific brain regions like the cranial, intracranial, and encephalic areas for subsequent geometric analysis. For this, image processing and transformation techniques for polar coordinates are used, followed by methods of determination of contours. The contours are approximated using a FS, and the coefficients are determined through a weighted least squares estimator. This estimator takes into account the feasibility of each point belonging to the contour, with lower weights indicating that the point is unlikely to be part of the contour. The main contributions of this paper include:

1. Identifying contour points along with their feasibility assessment.
2. Employing a FS to approximate the contour points.
3. Application of a weighted least squares estimator for the FS estimation, where weights represent the feasibility of the points.

Besides this introduction, this paper is structured as follows: Sect. 2 presents the image pre-processing methods employed to enhance the image quality, defines

the coordinate frame and illustrates the conversion from cartesian to polar coordinates and introduces the FS. while Sect. 3 describes the weighted least squares estimator, also explaining how it is used to estimate the contours. Furthermore, the process of determining the contour points and assigning their respective feasibility weights is elaborated upon in this section. In Sect. 4 a comprehensive presentation and discussion of the results is provided. Finally, in Sect. 5, the appropriate conclusions of the study and some directions for future work are presented.

2 Background

2.1 Image Pre-processing Techniques

Image processing involves utilizing several techniques and algorithms to improve analysis and extract meaningful information from digital images. Prior to image analysis, preliminary pre-processing steps are essential. Image enhancement aims to elevate image quality, ultimately to be evaluated by a human observer. In general, it works on the grayscale of the image, transforming it to increase contrast or highlight a particular area of interest [11].

In this project, whether the image has three color channels (RGB), it is converted to gray scale using the following formula for each pixel:

Grayscale Intensity = 0.2989 * Red + 0.5870 * Green + 0.1140 * Blue, with these weightings based on standard coefficients used in the ITU-R BT.601 recommendation, which specifies the luminance values for standard-definition television [12]. Then, a contrast adaptation is also applied to the image. Often, the organization of an image as a pixel matrix form is done in a square symmetry, which is due to the easiness of electronic implementation, whether of acquisition or image visualization systems [11]. Image filtering, prevalent in image processing, aims to bolster image quality, eliminate noise, emphasize key features, and smoothen the image. Within this assignment, a median filter is applied, this filter replaces the values of each pixel in the image by the median of the values of the pixels that are in the neighborhood of that pixel, to make image analysis easier.

2.2 Polar Coordinates

TIn a two-dimensional plane, polar coordinates are denoted as (r, θ) and describe the position of a point in the plane relative to a reference point, where:

$$x = r \cdot cos(\theta) \tag{1}$$

$$y = r \cdot sin(\theta) \tag{2}$$

In the cartesian plane, the position of a point is represented by the (x, y) coordinates. To convert these cartesian coordinates (x, y) to polar coordinates (r, θ), only two parameters are needed as given by the following expressions:

$$r = \sqrt{x^2 + y^2} \tag{3}$$

$$\theta = atan2(y, x). \tag{4}$$

In Eq. (3), $atan2(y, x)$ represents the arctangent function of two arguments taking into account the sign of the arguments to determine the correct quadrant of the angle θ. These expressions are used to convert a point in the two-dimensional cartesian plane (x, y) to polar coordinates, where r represents the radial distance from the point to the reference point (usually the origin) and θ is the angle formed between the segment connecting the reference point to the point in question and the positive x-axis, measured counterclockwise.

Initially, it is observed that the regions of the brain have an approximately circular shape, despite having deformations. For this reason, the image, originally in the cartesian coordinates (x, y), is converted to polar coordinates $(radius, angle)$. The center of mass of the image is taken as the origin of the polar coordinates reference frame and is calculated from the values of the pixels and their coordinates X and Y. These coordinates are determined from outside to inside. By converting the cartesian coordinates to polar, it is possible to represent the points of the image in terms of radius and angle, simplifying the analysis process and allowing the application of specific techniques for circular contours.

2.3 Fourier Series

The Fourier Transform is a fundamental tool in both mathematics and engineering, facilitating the analysis of signals within the frequency domain. Applying this transform to images reveals features like textures, edges, straight lines, and periodic patterns, to name a few [13]. The FS decomposes a periodic function with period Θ_0 into a sum of constant and sinusoidal functions with periods $n\Theta_0$, $n = 1, \ldots, \infty$. A sinusoid with period $n\Theta_0$ is denoted as the n^{th} harmonic. FS can also be used to approximate a function $f(x)$ in the interval $x_{min} \leq x \leq x_{max}$. For this purpose, define the periodic function

$$\tilde{f}(x) = \begin{cases} f(x) & x_{min} \leq x \leq x_{max} \\ f(x + k\Theta_0) & x < x_{min} \text{ or } x > x_{max},\ k = \pm 1, \ldots \end{cases} \tag{5}$$

where $\Theta_0 = x_{max} - x_{min}$ and determine the FS of $\tilde{f}(x)$. If $x_{min} = -\pi$ and $x_{max} = \pi$, then $\Theta_0 = 2\pi$ and the following expression represents $f(x)$ as a FS:

$$f(x) = a_0/2 + \sum (a_n cos(nx) + b_n sin(nx)), \tag{6}$$

where $a_0/2$ is the average value of $f(x)$, a_n and b_n are the coefficients, and n represents the frequency of the sine and cosine terms. The coefficient a_0 , a_n and b_n are determined by integrating $f(X)$ multiplied by the appropriate sine or cosine function over one period (from $-\pi$ to π) and the dividing by π. Expressions (7), (8), and (9) are used to calculate these parameters.

$$a_0 = \frac{1}{2\pi} \int f(x)dx \quad \text{from } -\pi \text{ to } \pi \tag{7}$$

$$a_n = \frac{1}{\pi} \int f(x)\, cos(nx)dx \quad \text{from } -\pi \text{ to } \pi \tag{8}$$

$$b_n = \frac{1}{\pi} \int f(x)\, sin(nx)dx \quad \text{from } -\pi \text{ to } \pi \tag{9}$$

The sum of these terms, with varying frequencies n, represents an approximation of the original function $f(x)$.

In this work, the FS is used to approximate the points of the outer contour of an image, using a linear combination of sine and cosine functions, in order to obtain a closed oval curve representative of the shape of the image. The objective is to determine the outer contour of an oval-shaped binary image, as well as its ellipse and active points in polar coordinates. To achieve this, we utilize the FS to approximate the image pixels, leading to a mathematically expressed closed oval curve:

$$r = a_0 + \sum_{i=1}^{n} (a_i \cos(i\theta) + b_i \sin(i\theta)), \tag{10}$$

where (r, θ) are the polar coordinates of the pixel. This expression calculates the radius of the pixels based on its angles. The number of terms in the series determines the accuracy of the approximation.

3 Weighted Least Squares Method

The Least Squares Method aims to estimate the parameters of a function by reducing the sum of the squared errors from a set of point measurements associated with that function. Hence, given a set of data points $(\theta_1, r_1), \ldots, (\theta_N, r_N)$, and a function $f(\theta, \alpha)$, where α are the unknown parameters, the least squares method estimates α by

$$\hat{\alpha} = \min_{\alpha} \sum_{i=1}^{N} \left[r_i - f(\theta_i, \alpha) \right]^2 . \tag{11}$$

Equation (10) can be rewritten as

$$r = \varphi(\theta)\alpha \tag{12}$$

where $\varphi(\theta) = \begin{bmatrix} 1 \cos\theta \sin\theta \ldots cos(n\theta) \sin(n\theta) \end{bmatrix}$ and $\alpha = \begin{bmatrix} a_0\ a_1\ b_1 \cdots a_n\ b_n \end{bmatrix}^T$. Hence $f(\theta, \alpha)$ is a linear function of α and the Least Squares estimate of α is [14]

$$\hat{\alpha} = \left(\Phi^T \Phi \right)^{-1} \Phi^T Y, \tag{13}$$

where

$$\Phi = \left[\varphi(\theta_1) \cdots \varphi(\theta_N)\right]^T \tag{14}$$

$$Y = \left[r_1 \cdots r_N\right]^T. \tag{15}$$

The Weighted Least Squares Method is an extension of the common Least Square Method, which is used to fit a curve to a data set. The main difference between the two methods is that the Weighted Least Squares Method assigns different weights to the data points based on their reliability [15] or, in this case, their feasibility. It estimates α by [14]

$$\hat{\alpha}_w = \min_{\alpha} \sum_{i=1}^{N} \left\{w_i(\theta_i)\left[r_i - f(\theta_i, \alpha)\right]\right\}^2, \tag{16}$$

where $w_i,\ i = 1, \ldots, N$ are the weights. $\hat{\alpha}_w$ is given by [14]

$$\hat{\alpha}_w = \left(\Phi^T W^2 \Phi\right)^{-1} \Phi^T W^2 Y, \tag{17}$$

where

$$W = \begin{bmatrix} w_1(\theta_1) \cdots & 0 \\ \ddots & \\ 0 & \cdots w_N(\theta_N) \end{bmatrix} \tag{18}$$

The weight of each point (r_i, α_i) is given by

$$w(\theta) = \exp\left[-\frac{\Delta_r^2(\theta)}{Q(\theta)}\right], \tag{19}$$

where $Q(\theta)$ the number of normalized pixels in the direction of θ and

$$\Delta_r(\theta) = r_{max}(\theta) - r_{min}(\theta) - \overline{r}(\theta) \tag{20}$$

with $r_{max}(\theta)$, $r_{min}(\theta)$ and $\overline{r}(\theta)$ being the maximum, minimum and median of the radius in the direction of θ.

The weight assigned to each point considers both the quantity of normalized pixels and the deviation of the difference between the maximum and minimum radii from the median. When the difference between the maximum and minimum radius equals the median, the weight has its maximum value equal to 1. This suggests that the point holds considerable significance in the overall analysis. However, if the difference between the maximum and minimum radius exceeds the median, the weight tends to approach zero. This implies that although these points are not entirely ignored, their contribution to constructing the harmonics is practically negligible in real terms.

3.1 Determination of Contour Points

It was created a function that takes a binary image (BW), the center of mass (CM), the type of mask (tm), and the order of the sinusoidal approximation (p) as inputs. The mask is designed to generate a final result where the interior is transparent and the exterior is opaque. The choice of the sinusoidal approximation order depends on the desired level of accuracy and the specific region to be segmented. Based on our analysis, a second-order FS sufficiently represents the skull. However, the intracranial and cephalic regions necessitate an eighth-order FS for precise modeling. The function returns multiple results, including the mask (M), the harmonic weights for the three lines (inner, middle, and outer) (W), the center of mass (CM), the polar coordinates of the contours (TC, RC), the polar coordinates of the outer boundary of the image (TC, RM), and the polar coordinates of the active points (TR, RR). Initially, the function prioritizes selecting white pixels to avoid processing the entire image unnecessarily. Subsequently, the polar coordinates are calculated using the center of mass, while also determining the radius of the farthest pixel in the desired angular direction. Furthermore, auxiliary variables such as 'a' (angle) and 'Q' (number of pixels found) are assigned for each internal angular value ranging from $-179º$ to $180º$.

When applying this function to the image, a graphical representation of its polar coordinates is generated, where the gray color represents the cranial and encephalic parts, while the white color represents the empty areas. Afterwards, the pixels with the maximum radius in the outermost part of the skull are identified for each angle. Next, by assessing the vertical variations, minimum values are ascertained, marking the point where the spherical coordinates graph shifts from gray to white. However, due to potential imperfections in the margins, there may be instances where the maximums and minimums are not precisely located. The presence of a "hole" is indicated if two successive points possess a radius exceeding 1. The weight calculation reduces the contribution of inaccurately determined points, resulting in a more precise representation of the contours.

4 Results

The method was applied to MRI scans of three distinct brains. One image was sourced from the WEB (Fig. 1(a)), while the others were from a dataset obtained from KAGGLE [16], consisting of a collection of cancer-free images (Fig. 1(b) and 1(c)). The objective of the analysis was to accurately assess the geometric characteristics of the brain region in these images. The analysis results are presented below. In the preliminary analysis, it is clear that all three brain regions exhibit a nearly oval shape. Figures 2, 3 and 4 depict the intermediate steps involved

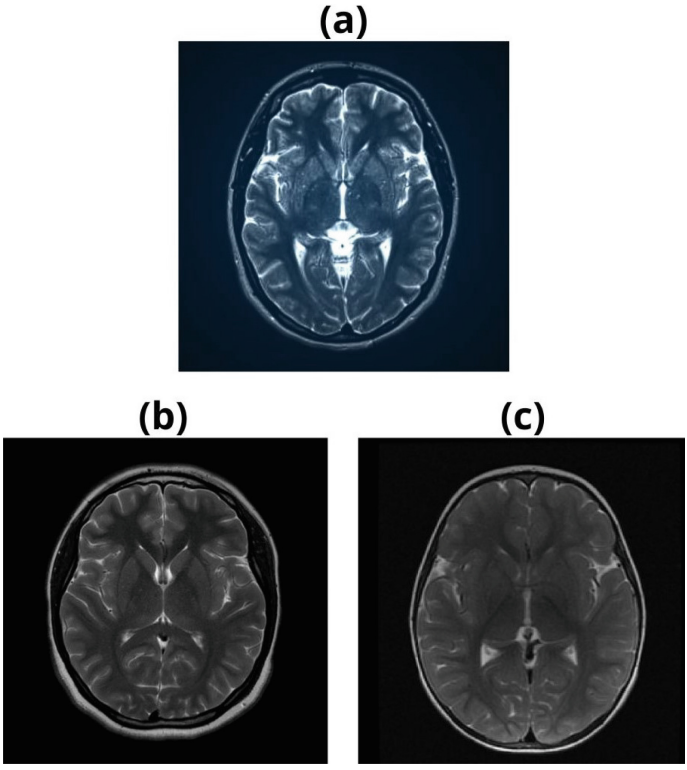

Fig. 1. Original MRI of the brains' horizontal section. (a) Example 1, (b) Example 2 and (c) Example 3.

in contour determination. They display the polar coordinates of the three brain images, highlighting all the determined contours obtained through the proposed method.

Figure 2 provides a visual representation of the outer and inner contours in the cranial region of the three analyzed MRI images. The outer contour is depicted by the black points, while the inner contour represented by the blue points. Additionally, the corresponding contour lines are shown in magenta. The green line represents the median calculated from these sinusoidal curves, which denote the skull's inner and outer contours.

Figure 3 presents an inverted representation for improved analysis, where the gray points have been converted to white and the white points to gray. The figure emphasizes the internal and external contour points of the intracranial regions in the three brains analyzed. The external contours are depicted by

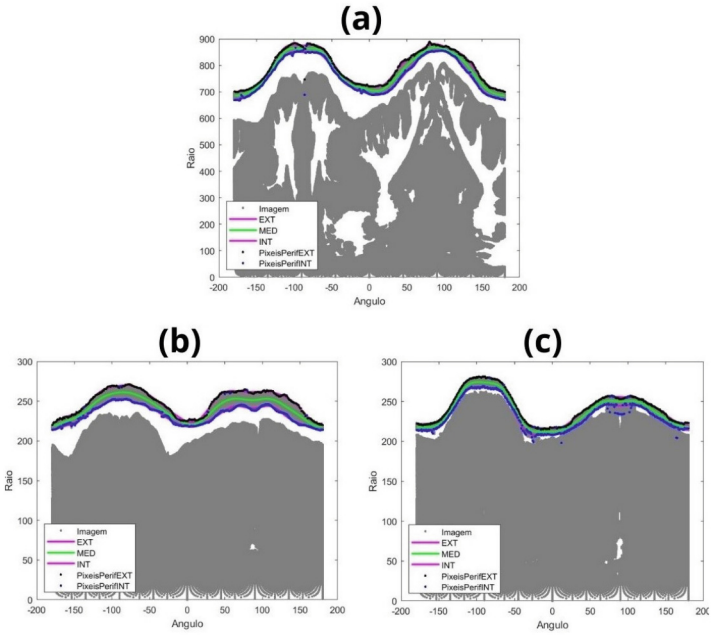

Fig. 2. Polar coordinate image of the external, middle, and internal contours of the skull for the three different images in Fig. 1, respectively, (a), (b) and (c).

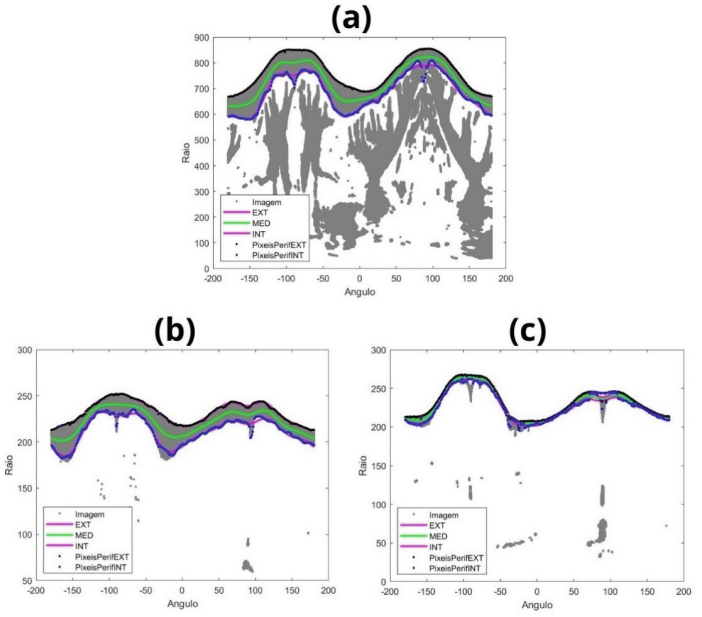

Fig. 3. Polar coordinate image of the outer, middle, and inner contours of the intracranial region for the three different images in Fig. 1, respectively: (a), (b) and (c).

Table 1. Geometric values of close curves.

Curve	Perimeter	Area	Asymmetry V/ H
(cranial) - outer	4997	1999418	8/ 11
(cranial) - middle	4903	1926315	6/ 9
(cranial) - inner	4810	1854696	6/ 10
(intracranial) - outer	4809	1853688	6/ 10
(intracranial) - middle	4567	1674084	11/ 13
(intracranial) - inner	4326	1504656	22/ 26
(encephalic) - outer	4340	1514347	22/ 25

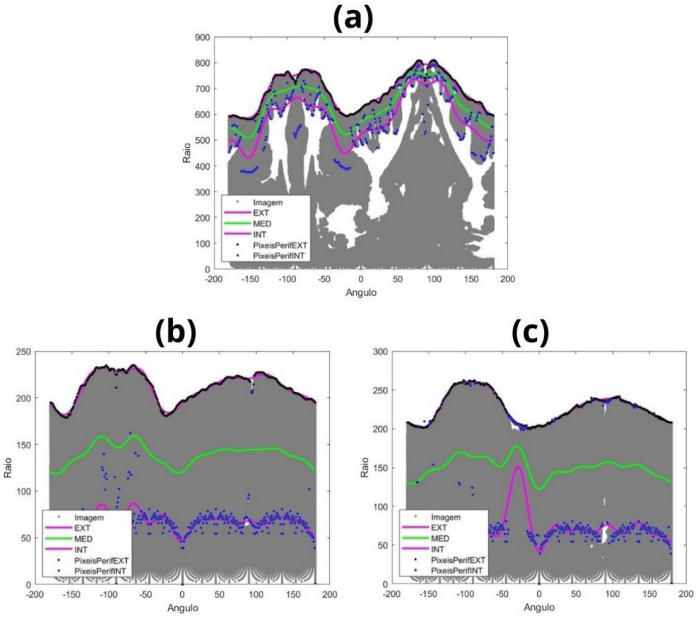

Fig. 4. Polar coordinate image displaying the outer, middle, and inner contours of the brain for the three different images in Fig. 1, respectively: (a), (b) and (c).

black points, while the internal contours are represented by blue points. The respective contours are illustrated by magenta lines. Furthermore, the green line represents the median.

Figure 4 illustrates the points corresponding to the external and internal contours in the encephalic region of the three analyzed brains. Black points represent the outer contour, and the inner contour is denoted by blue points. The respective contour lines are shown in magenta. The green line represents the calculated median of these points. However, in this specific region, it is not

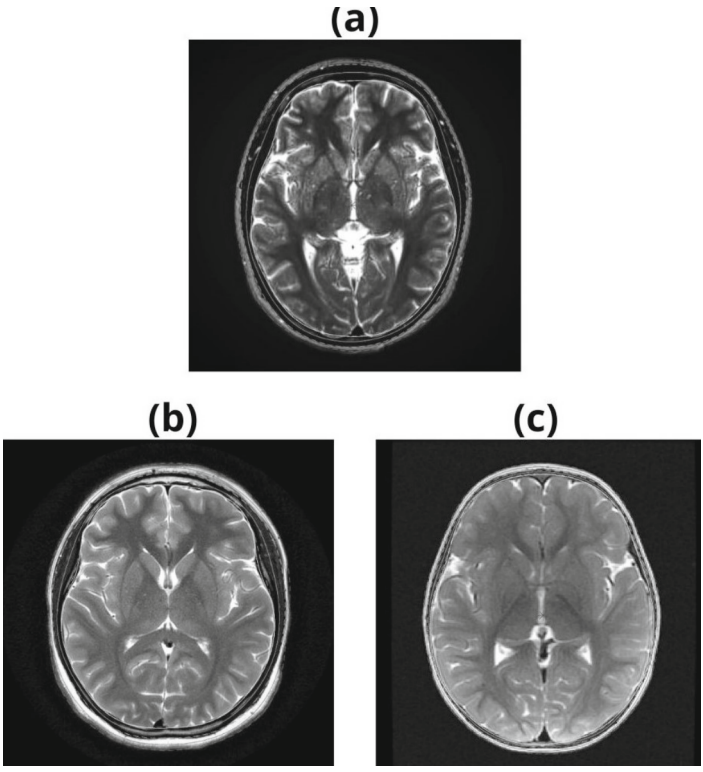

Fig. 5. Image of the brain with the center of mass indicated, as well as the determined contours of the different brain regions for the three different images in Fig. 1, respectively: (a), (b) and (c).

possible to accurately determine the lower points and the median due to its "closed" nature, which means that it lacks minimum points.

Figure 5 displays all the calculated contours in the respective brain images, along with the determined center of mass, which is essential for the calculation of the polar coordinates.

Figure 6 shows the masks constructed for the segmentation of each brain region. Mask 1 corresponds to the skull contour, mask 2 corresponds to the intracranial contour and mask 3 corresponds to the brain contour.

Finally, the values of perimeter, area, and vertical and horizontal asymmetry of each image were calculated, and the results can be found in Table 1. The first three rows of the Table 1 contain the values of the geometric parameters of the skull region, the next three rows represent the parameters of the intracranial region and the last row represents the parameters of the encephalic region. The closed lines of the contours have a length, *Perimeter*, and delimit a region with a certain area, *Area*. The asymmetry factor is a measure of the asymmetry with respect to an axis of symmetry. This factor is determined by averaging the modulus of the difference in distances between symmetrical pixels on the contour

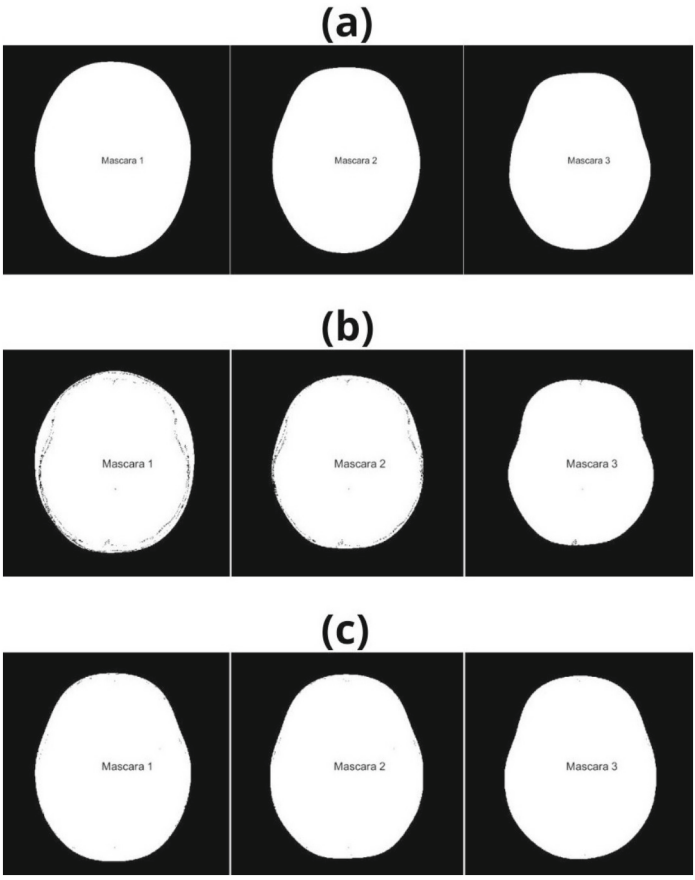

Fig. 6. Generated masks derived from the previously determined contours of the brain regions for the three different images in Fig. 1, respectively: (a), (b) and (c).

and the axis line. In this work, the axes of symmetry are lines containing the centre of mass of the image and the horizontal (H) or vertical (V) orientation. Both perimeter and asymmetry are given in pixels, while area is expressed in square pixels.

5 Conclusion and Future Work

This study demonstrates the feasibility of the use of mathematical models and techniques in the implementation of a method for geometric analysis of medical images, particularly of the brain MRI scans, in view to accurately determine the external and internal contours, as well as some parameters such as the perimeter, area and vertical and horizontal asymmetry of each image. The findings are synthesised in the figures showcasing the identified points of the contours in different brain regions, as well as the calculated contours and corresponding masks for segmentation.

The proposed method, resulting from a geometric approximation of the problem by means of the FS, is a novelty in the segmentation of brain MRI images.The results show potential to improve future brain MRI analysis and contribute to our comprehension of the geometry of different brain regions and tumors. However, for a robust validation of its potential, analyzing a larger set of images is essential. Furthermore, our approach will be bench-marked against other segmentation techniques for brain MRIs, such as edge detection, snakes, level-set methods, among others, or the rapidly emerging field of Convolutional Neural Networks (CNNs) for segmentation.

Acknowledgment. We would like to thank the reviewers for their careful reading and many suggestions that contributed enormously to the improvement of the paper.

References

1. Marreiros, F.M.M.: Análise e Interpretação de Imagem Médica com o apoio de Agentes de Software, Master's thesis, Universidade do Minho, Portugal, 2006
2. Ritter, F., et al.: Medical image analysis. IEEE Pulse **2**(6), 60–70 (2011)
3. Martins, L.G.: Volumetria de Estruturas Cerebrais Profundas com Imagem RM, Master's thesis, Universidade de Aveiro, Portugal (2018)
4. Wei, L., et al.: An fMRI study of visual geometric shapes processing. Front. Neurosci. **17**, 1087488 (2023)
5. Covolan, R., Araujo, D.B.D., Santos, A.C.D., Cendes, F.: Ressonância Magnética Funcional: As funções do cérebro reveladas por spins nucleares. Ciência e Cultura **56**(1). São Paulo, Brasil (2007)
6. Azmoun, S., et al.: Cognitive impact of exposure to airborne particles captured by brain imaging. Adv. Neurotoxicol. **7**, 29–45. Elsevier (2022)
7. Rajchl, M., Ktena, S.I., Pawlowski, N.: An Introduction to Biomedical Image Analysis with Tensorflow and DLTK, July 2018. https://blog.tensorflow.org/2018/07/an-introduction-to-biomedical-image-analysis-tensorflow-dltk.html
8. Bear, M.F., Connors, B.W., Paradiso, M.A.: Neurociências: desvendando o sistema nervoso. Artmed editora (2002)
9. VanPutte, C., Regan, J., Russo, A.: Anatomia e Fisiologia de Seeley- 10a Edição. McGraw Hill, Brasil (2016)
10. Agostinho, E.T.: Estudo da Evolução de Tumores Cerebrais, Master's thesis, Faculdade de Ciências e Tecnologias da Universdidade do Algarve, Portugal, 2007
11. de Albuquerque, M.P.: Processamento de Imagens: Métodos e Análises, Centro Brasileiro de Pesquisas Físicas MCT, 2000
12. BT, R., et al.: Studio encoding parameters of digital television for standard 4: 3 and wide-screen 16: 9 aspect ratios. International Radio Consultative Committee International Telecommunication Union, Switzerland, CCIR Rep (2011)
13. Pupin, J.R., Silva, K.S., Carbone, V.L.: Introdução às Séries e Transformadas de Fourier e Aplicações no Processamento de Sinais e Imagens. Trabalho (Conclusao de Curso)-Universidade Federal de Sao Carlos, Sao Carlos (2011)
14. Goodwin, G.C.: Dynamic system identification: experiment design and data analysis. Math. Sci. Eng. **136** (1977)
15. Weisberg, S.: Applied Linear Regression, 4th edn. Wiley, Hoboken (2014)
16. Chakrabarty, N.: Brain MRI Images for Brain Tumor Detection (2019). https://www.kaggle.com/datasets/navoneel/brain-mri-images-for-brain-tumor-detection